Sensors and Actuators B 255 (2018) 843–853

Contents lists available at ScienceDirect

Sensors and Actuators B: Chemical

journal homepage: www.elsevier.com/locate/snb

Research Paper

Methane detection scheme based upon the changing optical constants of a zinc oxide/platinum matrix created by a redox reaction and their effect upon surface plasmons

Thomas Allsop[a,*], Vojtěch Kundrat[b], Kyriacos Kalli[c], Graham B. Lee[a], Ron Neal[d], Peter Bond[d], Baogul Shi[e], John Sullivan[e], Phil Culverhouse[d], David J. Webb[a]

[a] Aston Institute of Photonic Technologies, Dept. of Electronic Engineering, Aston University, Birmingham, B4 7ET, UK
[b] Nanoscience Research Group, School of Engineering and Applied Science, Aston University, Aston Triangle, Birmingham, B47ET, UK
[c] Department of Electrical Engineering, Computer Engineering and Informatics, Cyprus University of Technology, Limassol 3036, Cyprus
[d] School of Computing, Communications and Electronics, University of Plymouth, UK
[e] Midlands Surface Analysis Ltd, Aston University, Birmingham, B4 7ET, UK

ARTICLE INFO

Article history:
Received 8 March 2017
Received in revised form 25 July 2017
Accepted 7 August 2017
Available online 23 August 2017

Keywords:
Localized surface plasmons
Metal oxide semiconductors
Optical sensing
Gas sensing
Fibre optics

ABSTRACT

We detect changes in the optical properties of a metal oxide semiconductor (MOS), ZnO, in a multi-thin-film matrix with platinum in the presence of the hydrocarbon gas methane. A limit of detection of 2% by volume with concentrations from 0 to 10% and maximum resolution of 0.15% with concentrations ranging from 30% to 80% at room temperature are demonstrated along with a selective chemical response to methane over carbon dioxide and the other alkane gases. The device yields the equivalent maximum bulk refractive index spectral sensitivity of 1.8×10^5 nm/RIU. This is the first time that the optical properties of MOS have been monitored to detect the presence of a specific gas. This single observation is a significant result, as MOS have a potentially large number of target gases, thus offering a new paradigm for gas sensing using MOSs.

1. Introduction

Metal oxide semiconductors (MOS) have been widely researched for their possible application to the field of gas sensing; in particular, the detection of toxic and explosive gases in air such as carbon monoxide and methane [1,2]. MOS sensors have been shown to have advantages over more conventional spectroscopic techniques that rely on the measurement of absorption features [3]; such as lower fabrication costs, miniaturisation, integration and multiplexing capabilities. The downside of MOS sensors are problems and issues related to stability and chemical selectivity along with their need to operate above ambient temperature, and as a result of their electrical operation there is the problem of spark hazards. Elevated temperature operation and sparking hazards are significant problems in the detection of methane and other potentially explosive gases [2,3].

The key chemical and physical properties of methane gas are that it is colourless, odourless, explosive, an asphyxiate and lighter than air. Monitoring the presence and concentration of methane is a major safety issue for a number of industries; for example, in coalmines, power plants, waste water treatment, landfill sites and the petroleum chemical industry [4]. Recently methane has achieved much greater prominence in the public domain because of its more significant role than carbon dioxide in the greenhouse effect [5].

There has been interest by researchers to develop non-electrical sensing technologies, to address the aforementioned issues. Spectroscopic techniques have been explored [4,6,7] in the telecommunications wavelength range from 1300 nm to 1700 nm. These spectroscopic sensing platforms operate very well as individual units but have several drawbacks, for example, spark hazard from peripheral and drive electronics in standalone units, their robustness in extreme environments, difficulties in multiplexing these type of sensors to form a sensing array and their relatively high cost to produce. There are other problems with spectroscopic techniques, such as the typically used absorption lines of methane (1330 nm, 1667 nm) having a natural linewidth far narrower than the majority of the telecommunications laser modules including distributed feedback lasers (DFBs); typically an unmodulated CW DFB laser has a linewidth is of a few MHz, which can result in a very small intensity variation even for relatively large gas concentrations. There are solutions to this particular problem, using

* Corresponding author.
E-mail addresses: t.d.p.allsop@aston.ac.uk, allsotdp@aston.ac.uk (T. Allsop).

http://dx.doi.org/10.1016/j.snb.2017.08.058

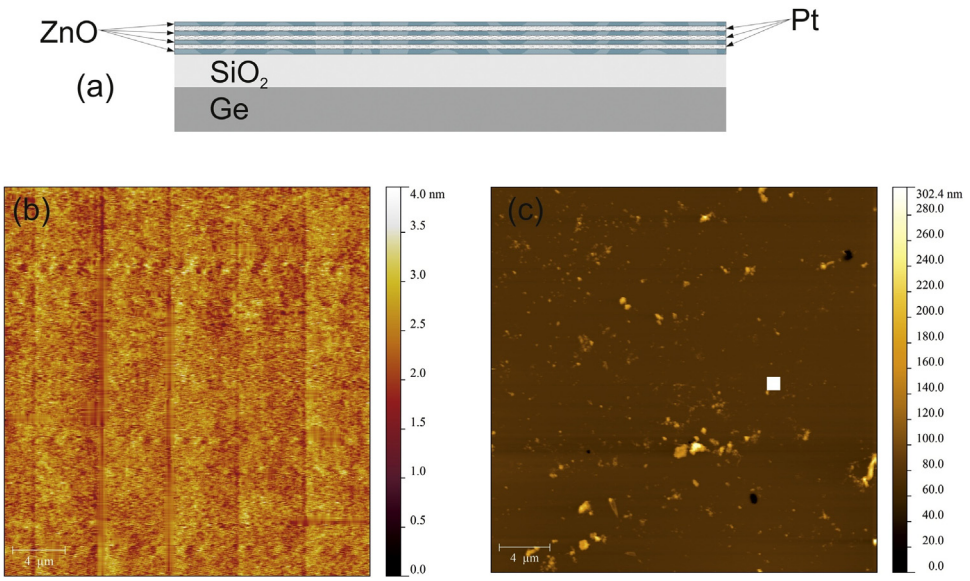

Fig. 1. (a) Schematic of the sequence of deposition of the layers that make up the thin film coating, with thickness of germanium (48 nm), silicon dioxide (48 nm), platinum (3 nm) and zinc oxide (3 nm). AFM image and topological data before (b) and after (c) UV-laser processing of a typical thin film device as described above.

modulated lasers and the technique called derivative spectroscopy [7] but this increases the complexity of the gas sensing systems and can lead to an increase in possible errors from random spectral artefacts created by the sensing scheme. It also requires a greater degree of stabilisation, as well as the use of 2nd or 3rd order phase servo-control schemes. Moreover, there are over a hundred absorption lines and there are many adjacent rotational absorption lines corresponding to each major absorption band that all have a temperature dependence [8,9], which can make for difficult interpretation; humidity interference can be an additional problem [1]. For lasers that have linewidths of 10 MHz, their coherence lengths are of the order of tens of metres, therefore multiple reflections within the sample test absorption cell itself can produce significant effects upon the transmission/absorption spectra. Another gas sensing approach – gas chromatography – can perform an accurate quantitative analysis of the presence of methane gas, but it is expensive and unsuitable for in situ monitoring, which is essential in most cases [10,11].

Other types of optical fibre methane gas sensors that are not based upon spectroscopy have received significant attention and are being explored because of their remote detection capability, safety in hazardous environments (potential ambient or low temperature operation), multiplexing capabilities, low cost, small footprint, non-spark (optical not electrical) property and immunity to electromagnetic radiation. These devices lend themselves to applications in the deep seam coal mining environments, where there is a possibility of methane accumulation [4]. The fibre-optic type of sensor has met with some success but still has major problems that need to be addressed; a few of their shortcomings are pointed out below. Several configurations have been investigated, for example an optical fibre intra-cavity within a single mode fibre or using poly-crystalline- optical fibre [12,13]; an interferometric device, which operates in a manner similar to the aforementioned [4,6,7] spectroscopic technique and thus displays similar problems [12,13]. Furthermore, evanescent field sensors have been used in the past [14], but measure only changes in the bulk refractive index, therefore chemical selectivity is an issue. Moreover, other optical fibre sensors, such as long period grating devices have been considered, working in conjunction with zinc oxide films to make the sensors chemically specific to methane but these need to operate at temperatures in excess of 200 °C [15]. To lower this higher operating temperature researchers have investigated using a palladium–silver-activated ZnO surface, however this still requires operation at temperatures in excess of 100 °C [16].

In this paper we present an optical sensing platform that is based on metal oxide semiconductor technology, but that monitors changes in the material properties of the MOS optically. This material and coating architecture is capable of selective sensing of methane gas using zinc oxide by producing a distinct and measurable wavelength shift, which is opposite in sign to that produced by changes in the bulk refractive index. This spectral behaviour is underpinned by a mechanism that is based upon the interaction of near infrared localised surface plasmons generated by platinum regions within a matrix of zinc oxide. The optical device also has multiplexing capabilities and can be used in hostile or explosive environments and has the potential to be used in gas sensing applications. The optical MOS sensor has a methane limit of detection of 2% by volume, at low concentrations of methane, ranging from 0 to 10% by volume with a best detection performance of 0.15% around concentration values of 50%. The device produces a non-linear response and yields a resolution of 0.4% over concentrations of 85.0% of methane in air, at room temperature and at ambient pressure. The typical sensitivity of the device was 1.05 dB/fractional volume increase in methane.

2. Materials and methods

2.1. Fabrication and physical characterisation

The device is constructed in three stages [17]. Firstly, a standard single mode optical fibre (SMF-28) is mechanically lapped down to 3 μm ± 0.5 μm from the core-cladding interface. This distance is large enough to minimise the evanescent field strength at the flat of the lapped fibre surface and to stop the coated flat of the D-shaped acting as a “mode sink”, which would affect the overall dynamic range (optical power) of the sensor. Secondly, vacuum RF plasma sputtering is used to deposit a series of thin film coatings onto the flat region of the lapped fibre. Initially the fibre was coated with germanium (48 nm) and silicon dioxide (48 nm). These two coatings are followed by alternating layers of platinum (3 nm) followed by zinc oxide (3 nm). This layering process is repeated four times with an additional overlay of platinum (3 nm) (Fig. 1). Follow-

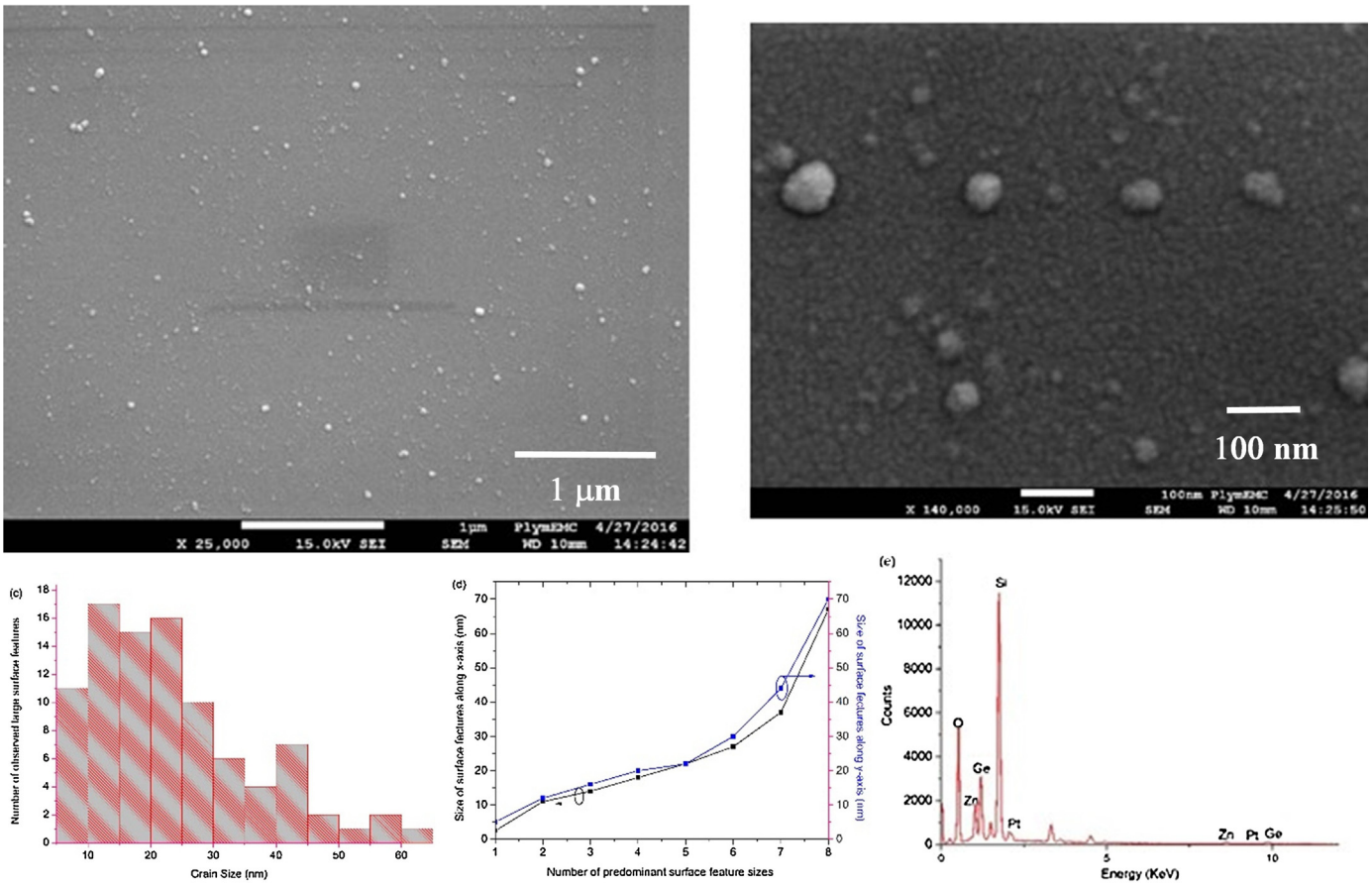

Fig. 2. Experimental results obtained from field-emission scanning electron microscopy on the Zn/Pt matrix coating (a) a typical large field view of the surface of the coating (b) a high resolution image of the Zn/Pt matrix coating surface (c) a typical histogram of the size distribution of the nucleation surface features. (d) the distribution of the sizes of the background granulation (e) a typical spectrum of the film coating.

ing the fabrication of the coatings, they are exposed to ultra-violet light (244 nm Sabre FreD Coherent laser) in the form of a diffraction pattern created from a phase mask and optical apparatus used in the fabrication of a conventional fibre Bragg grating [18]. These thin film coatings have been examined by several techniques during the fabrication process; below we present atomic force microscopy (AFM) images before and after UV processing (Fig. 1(b) and (c), respectively).

Analysing the AFM data, we observe an increase in the overall surface area in contact with the gases (Fig. 1), this has been estimated to 2.5% in area. The overall roughness for the non-exposed surface is 0.257 nm, which increases to 3.7 nm after exposure and the average heights increase from 2.4 nm to 74 nm. The non- UV processed material is flat and shows artefacts in the form of stitch errors from the AFM measurement itself (Fig. 1b). These changes in topology lead to the different spectral optical responses observed as a function of polarisation, bulk refractive index and the spectral response to the presence of methane. The holes that appear in the UV processed surface have a depth of about 70 nm, which is the combined thickness of the SiO_2 and the ZnO/Pt layers. Furthermore, the coatings were investigated using x-ray photon-emission spectroscopy (XPS) and field-emission scanning electron microscopy (FSEM) both with and without UV processing. The FSEM results before UV processing are shown in Fig. 2; inspecting Fig. 2(a) and (b) shows granulation of the surface of the coating along with surface nucleation of the thin film coating. The typical size distribution of key nucleation surface features is shown in Fig. 2(c), yielding a mean size of 22 nm and standard deviation of 13 nm. Furthermore, there is a finer background granulation of the majority of the surface caused by the fabrication procedure, ranging from 3 to 20 nm in size, see Fig. 2(d). The composition of the nucleation surface features and the background surface were investigated, and all physical features of the surface have the same composition and the same ratio of each component used in the ZnO/Pt matrix fabrication, see Fig. 2(e).

Due to the known physical dependences of surface plasmons, the MOS/Pt surface plasmons' polarisation dependences and the bulk refractive index spectral sensitivity were investigated using the apparatus shown in Fig. 3.

Investigating the polarisation dependency of the localised surface plasmon resonances through the UV processing there are several observations to be made. Firstly, surface plasmon resonances can occur over the available light source wavelength range (Fig. 4(a)), with excitation resonances of similar optical strength across the observable spectrum. The explanation for this large spectral tunability relates to the distribution of the platinum in the matrix coating. The fabrication procedure is only depositing the equivalent of 3 nm of material in one layer from the sputtering target. An individual layer initially forms islands of material before becoming a coating of uniform thickness after more material is deposited; this happens during the first few nanometers [19], see Fig. 2. This leads to a range of particle sizes of platinum that supports the surface plasmons, which are also dependent upon the material surrounding the platinum particles, which is either air or zinc oxide or both, and these plasmons are classified as localised surface plasmons [20]. Fig. 1(b) shows that the coating is relatively smooth (roughness ~ 0.3 nm); with this surface topology one may anticipate that the propagation length of the surface plasmon would be long, thus the full-width-half-maximum (FWHM) of the resonance

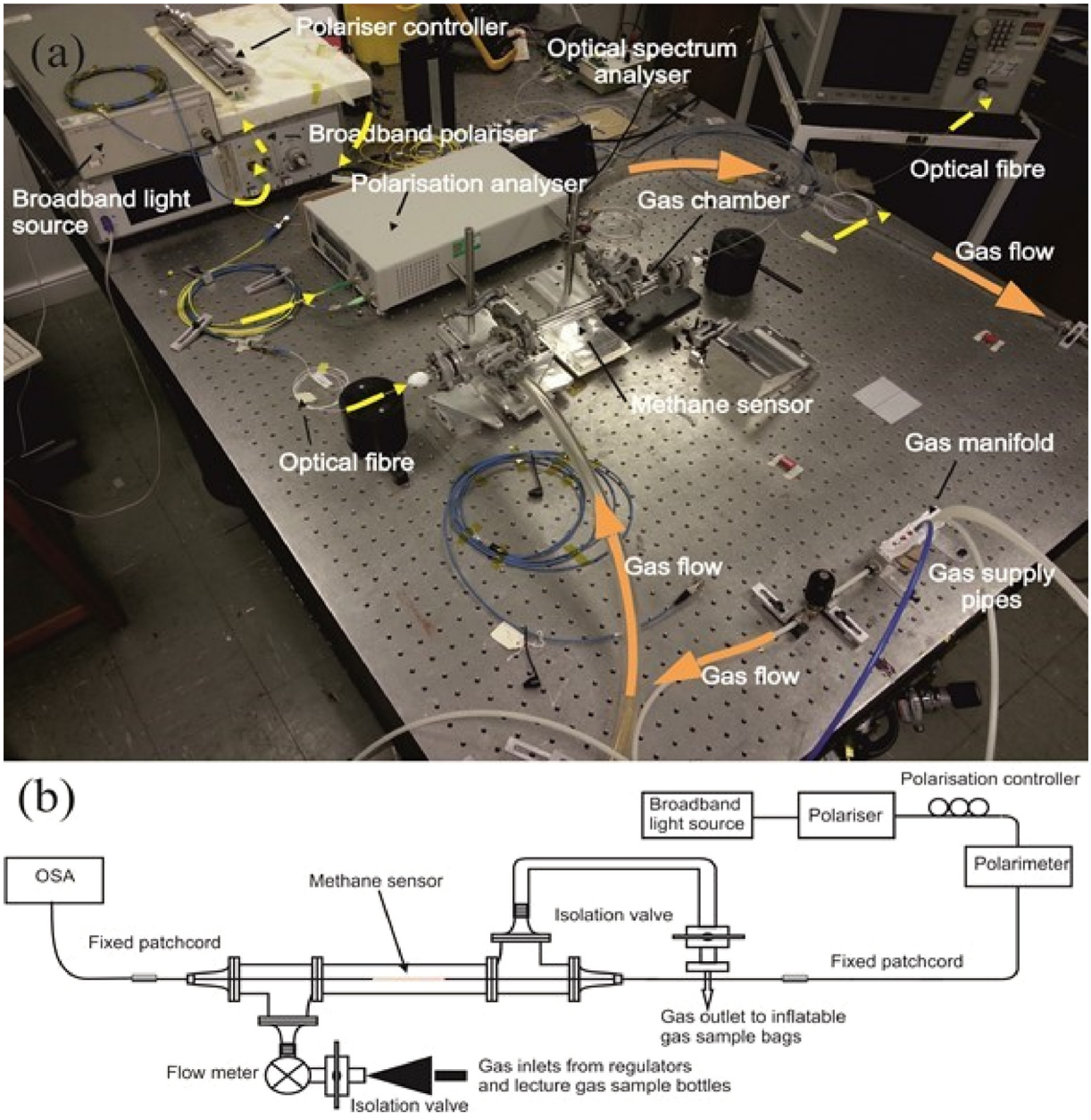

Fig. 3. (a) Apparatus used to investigate the polarisation and refractive index spectral sensitivities. (b) Schematic of apparatus used.

would be spectrally narrow [21,22]. Inspecting a typical resonance of the surface plasmon in transmission, e.g. those shown in Fig. 4(a), the FWHM is approximately 300 nm, indicating that the propagation length is actually small [23]. These values are an indication that this device is generating localised surface plasmons. Fig. 4(b) yields a polarisation sensitivity (rotating the azimuth of polarisation) of 2.7 $dBDeg^{-1}$ in close proximity to maximum optical strength of the resonance, which is similar to other localised surface plasmon fibre devices [17]. Fig. 4(c) is an illustration of how the dispersion properties of the surface plasmons change with wavelength; this spectral behaviour is expected and has been reported elsewhere [22].

3. Results

3.1. Spectral sensitivity and chemical selectivity

The bulk refractive index sensitivity of a device prior to UV inscription was investigated both in the gas and liquid regimes. Fig. 5 shows the spectral behaviour and spectral sensitivity of a typical device in the aqueous index regime, providing $\Delta\lambda/\Delta n$ of 3800 nm/RIU and $\Delta I/\Delta n$ of 230 dB/RIU from peak excitation measurements over an index range of 1.31–1.37; these are high sensitivity values compared to other devices [24].

The highest sensitivities occur in the low refractive index regime (gas phase) with a maximum bulk material refractive index spectral sensitivity of $\Delta\lambda/\Delta n \approx +3.7 \times 10^4$ nm/RIU. The change in the optical strength of the resonances was negligible, see Fig. 6. Inspecting Fig. 6, the gases used were the alkane gases and carbon dioxide at room temperature (23 °C) and with nominal pressure of one atmosphere. All the gases, with the exception of methane, demonstrated a consistent wavelength shift attributable to an increase in bulk refractive index. The spectral response of the sensor to methane is opposite to that for increasing bulk refractive index; all other gases produced a blue wavelength shift and methane produced a red wavelength shift from air, indicative of a specific chemical spectral response. Carbon dioxide (CO_2) has a similar bulk refractive index to

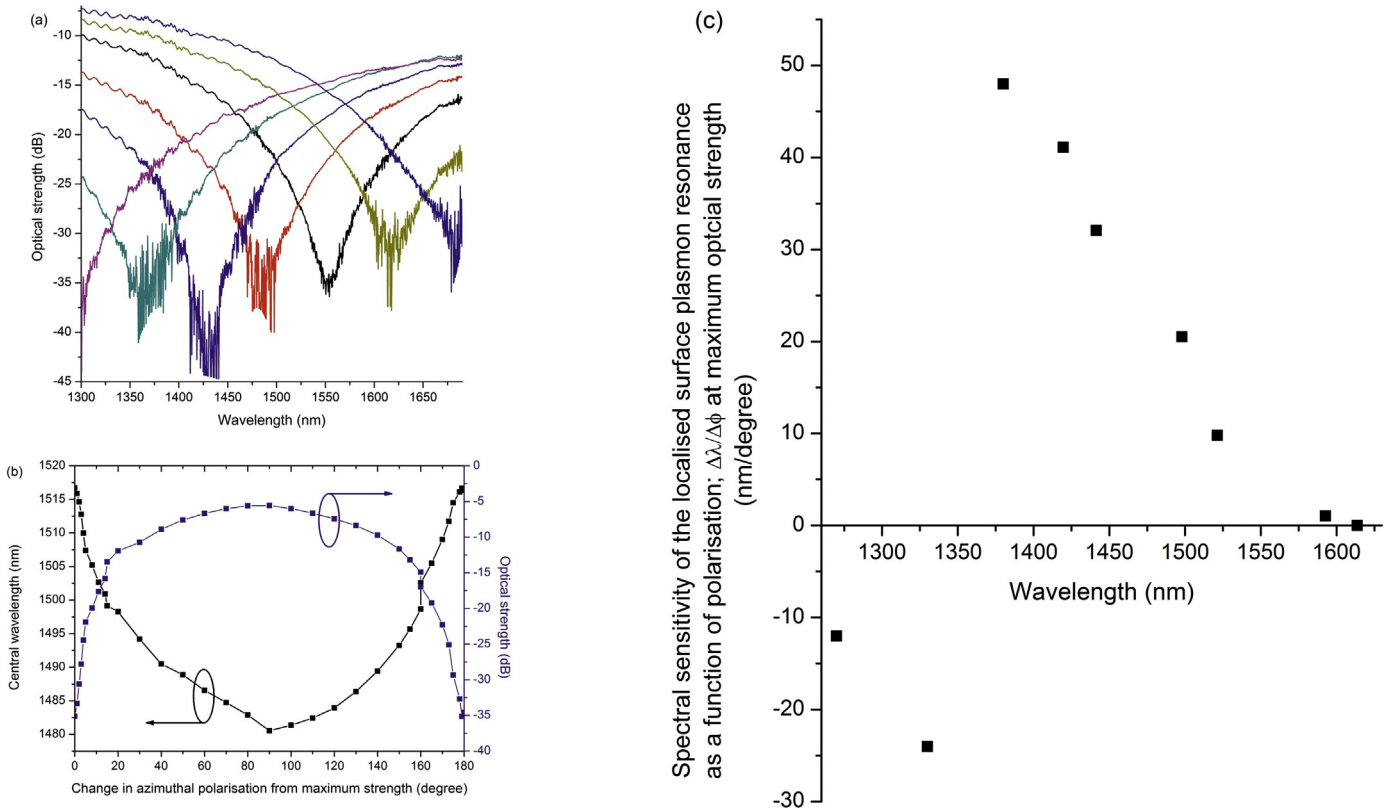

Fig. 4. (a) An example of the spectral dependence upon polarisation variation. (b) A typical variation of the wavelength and optical strength of a surface plasmon resonance from a maximum in coupling with respect to azimuthal polarisation. (c) The wavelength sensitivity as a function of polarisation at various spectral locations.

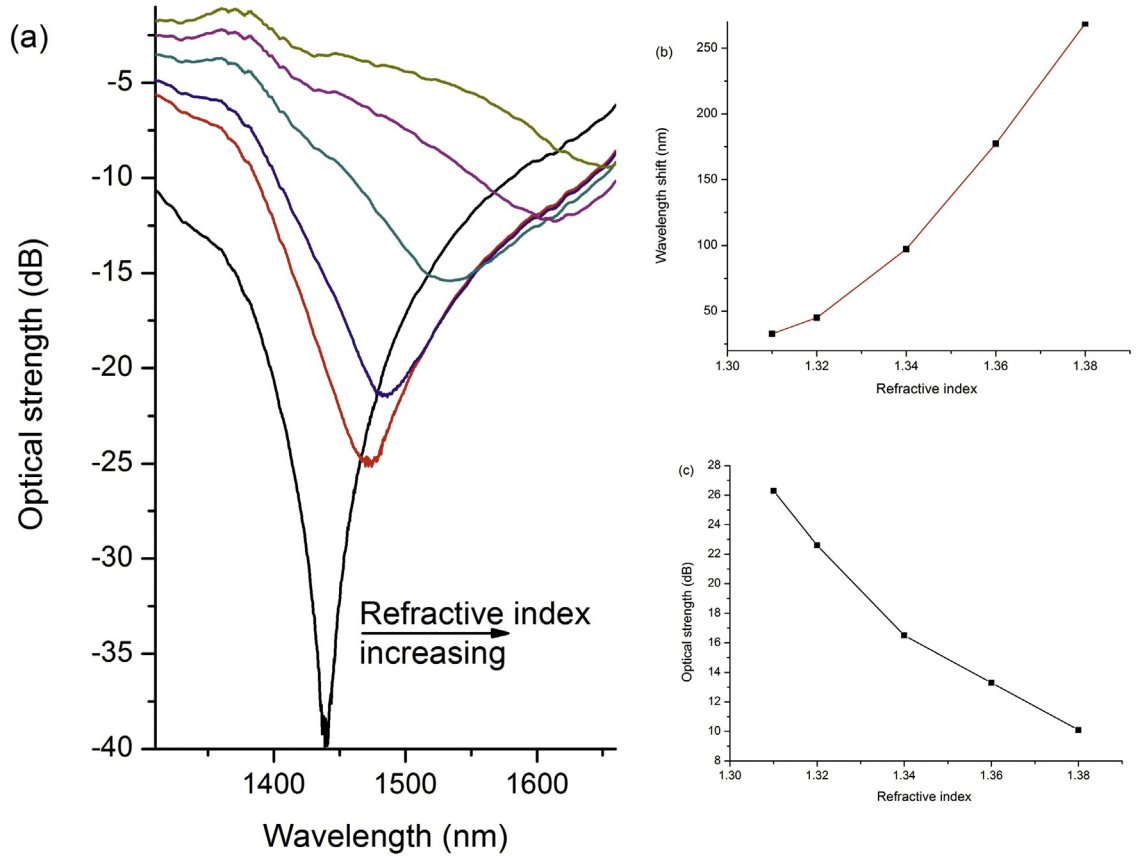

Fig. 5. (a) The transmission spectrum dependency upon changes in the surrounding refractive index in the aqueous regime; (b) and (c) the resonant wavelength shift and optical strength change (compared to device in air) as a function of refractive index, respectively.

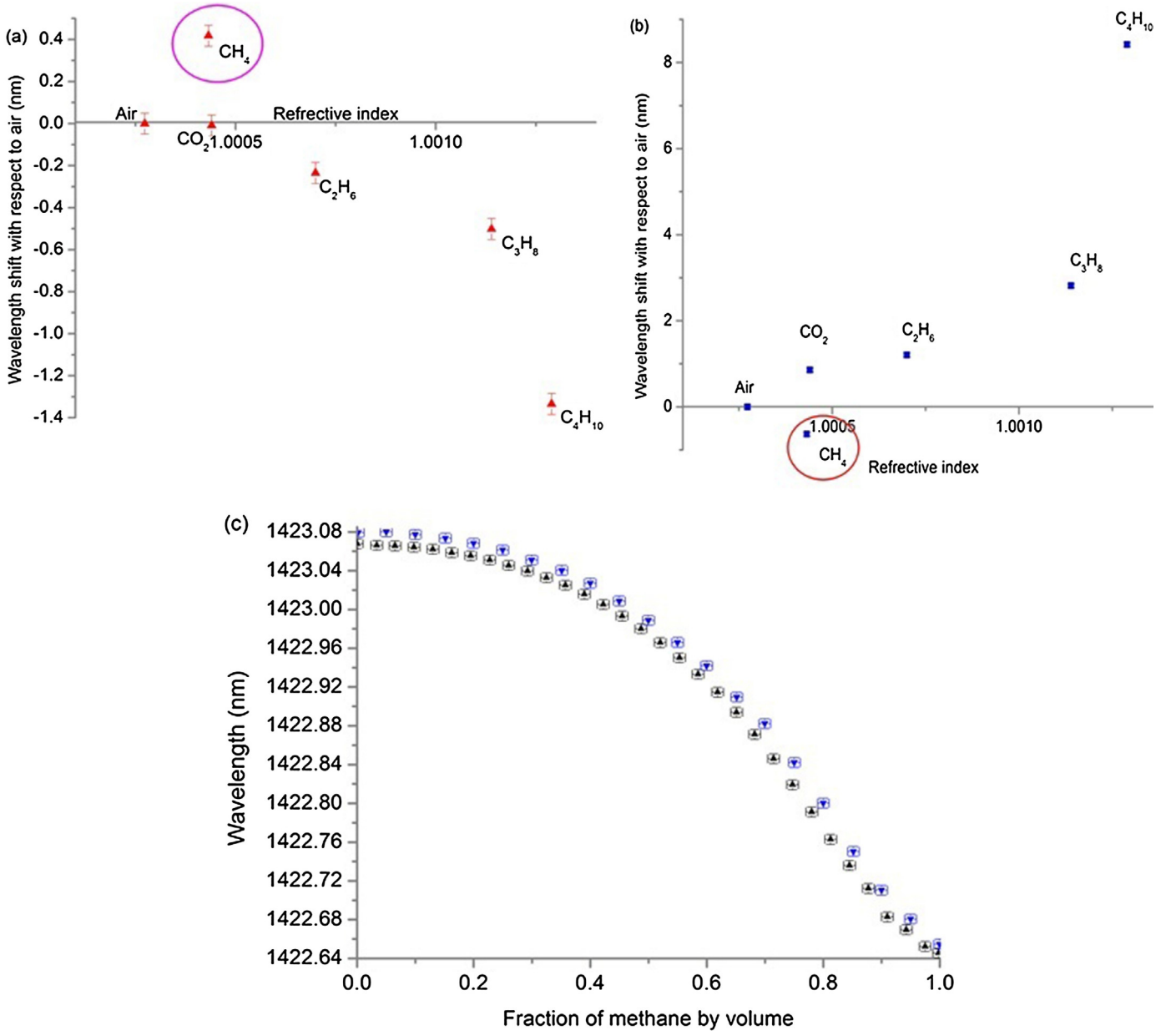

Fig. 6. Refractive index spectral sensitivity in the gas regime and the demonstration of a specific response to methane at two different wavelengths. (a) The initial wavelength is 1347 nm and (b) the initial wavelength is 1360 nm. (c) The wavelength shifts of the resonance as a function of methane concentration at 23. 0 °C and 25.7 °C with relative humidity of 50.60% and 43.10%, ▲ , ▲ .

methane under these conditions and at the wavelengths of interest (the refractive index at a wavelength of 1350 nm is approximately 1.0004401 [25] compared with an estimated bulk refractive index for methane of 1.000432 [26]). Therefore CO_2 was used to compare the bulk refractive index response.

It was found that the dispersion properties were different for localised surface plasmon resonances at differing spectral locations, thus environmental perturbation can cause red or blue wavelength shifts of the plasmon's resonance depending upon the spectral location of the resonance relative to the dispersion curve for a given localised surface plasmon. Therefore, experimentally we have studied two different surface plasmons and their resonances. The first displays an overall blue wavelength shift from air for increase in bulk refractive index with a resonance at 1348 nm with methane producing typical red shifts of +0.5 nm. At the longer wavelength at 1360 nm, the device displays an overall red wavelength shift from air for bulk increase in refractive index with methane producing typical blue shifts of −0.6 nm The equivalent bulk refractive index spectral sensitivity from carbon dioxide to methane is -1.8×10^5 nm/RIU for the surface plasmon resonance at the longer wavelength and $+4.1 \times 10^4$ nm/RIU at the shorter wavelength resonance.

Further experiments revealed that this sensing platform yielded a limit of detection of methane of 2% by volume at low concentrations. The spectral sensitivity varies non-linearly, at the lower concentrations from 0 to 12%, with maximum sensitivity occurring approximately in midrange concentrations with a resolution of 0.15% with decreasing spectral sensitivity at concentrations of 85.0% and above, which yielded an accuracy of 0.3% by volume, see Fig. 6(c).

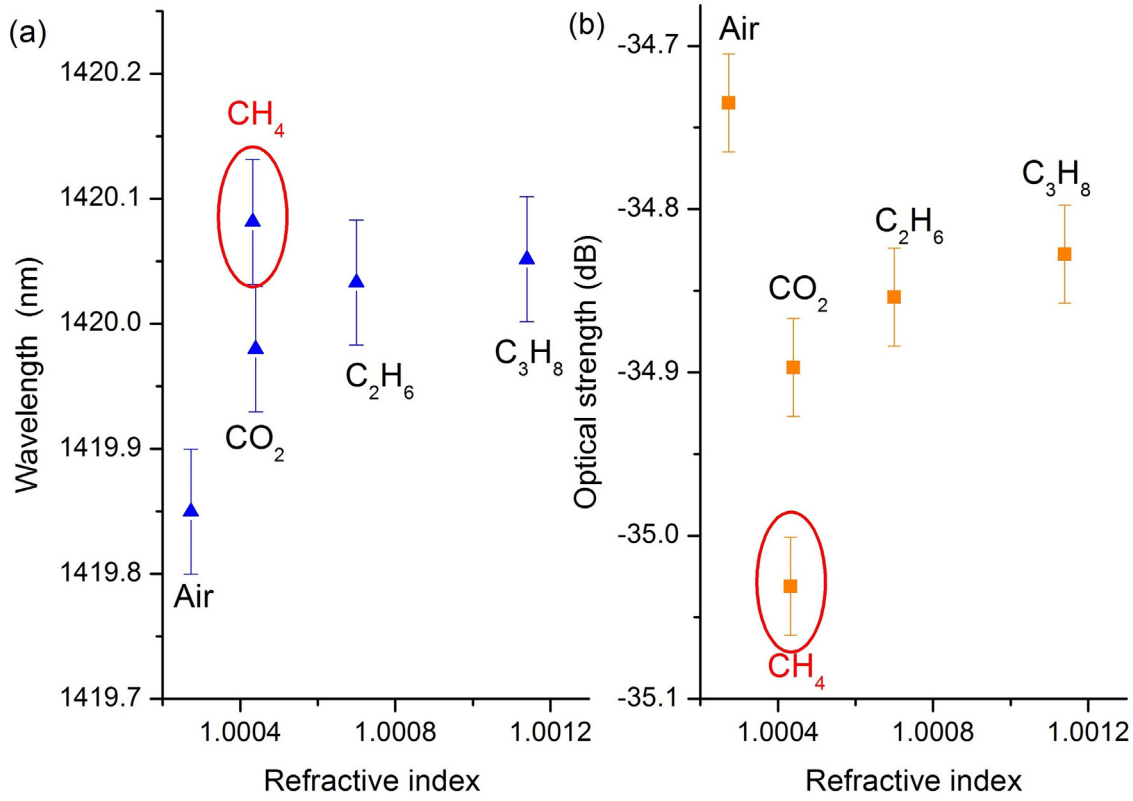

Fig. 7. A typical refractive index spectral sensitivity of the UV processed device in the gas regime.

It is known that Humidity effects the electrical properties of ZnO, in fact, ZnO electrical sensors are used to detect humidity [27]. The fact that humidity may have an effect on the sensing mechanism the experiment of methane sensitivity was repeated at different temperatures and thus different relative humidities ranging from a minimum temperature of 23.0 °C and humidity of 50.6% to 25.7 °C and relative humidity of 43.1%, The humidity appears not to significantly change the functionality of the sensors over the range investigated, but gives a small DC wavelength offset which is a blue wavelength shift, the same as the sensor's response in the presence of methane. This is due to the fact that water vapour has a lower refractive index than dry air, see Fig. 6c. The 7.5% relative humidity change produced a wavelength shift of ~0.02 nm over the full range limit detection; 0.44 nm.

Furthermore, the devices that were UV processed were also characterised; typical results are shown in Fig. 7, which are different to those of the non-UV processed sensors shown in Fig. 6. The change in spectral behaviour is expected due to the fact that the topology of the coating is different, as are the ratios of the elements exposed to the environment. Therefore the UV processing has transformed the structure into a different type of localised surface plasmon device [17], thus changing the spectral characteristics. These results are included to illustrate that the specific chemical mechanism providing a specific response to methane is still applicable to another sensing device configuration. Fig. 7 shows that methane yields a larger wavelength shift and change in optical strength than would be expected for a change in bulk refractive index. The UV processed devices yielded less overall spectral sensitivity in the gas regime of $\Delta\lambda\ /\Delta n = 380$ nm/RIU for bulk refractive index change. The highest spectral sensitivity observed for the UV processed devices is from methane to carbon dioxide, yielding the equivalent bulk refractive index spectral sensitivity of $\Delta\lambda\ /\Delta n = -1.3 \times 10^4$ nm/RIU and $\Delta I\ /\Delta n = 1.7 \times 10^4$ dB/RIU, which are considerably less than the non-UV processed sensing platforms.

However, the results shown in Fig. 6 suggest that the sensor's response to methane is not attributable to increase in bulk refractive index. Research has been conducted that suggests offers a possible mechanism to produce this distinct spectral behaviour of the surface plasmon device with methane.

It is believed that chemisorption of the oxygen on the surface of the MOS is the prime mechanism in changing the electrical properties of the MOS, such as conductivity, which has a relationship to permittivity and thus effective refractive index [28]. It is known that the electrical resistance of ZnO is dependent upon the adsorbed O_2 molecules on its surface. The oxygen molecule attracts an electron from the conduction band of ZnO (an n-type semiconductor) and forms O_2^-, this occurs at room temperature. These O_2^- ions get adsorbed on the ZnO surface forming ZnO:O_2^- species through strong ZnO–O_2^- interaction. It is known that addition of a metal atom to this system strips the O_2^- molecule from the ZnO [16]. There is evidence to suggest that the addition of platinum atoms in contact with ZnO produces Pt: O_2^- and like other such compounds [16] the bond becomes weaker and so the oxygen species is readily released from the metal atom; this can occur at low temperatures. It is known that methane breaks down into $C'H_3$ and $'H$ [29]. This hydrogen radical reacts with the absorbed O_2^- that has been coupled to the Pt, producing water (H_2O) and carbon dioxide (CO_2). Other experimentalists have shown that this type of reaction has a negative Gibb's Free energy [29]. Following this initial breakdown of the methane there is rapid total oxidation of methane with oxygen; this can occur at room temperature, indicated by the Gibbs free energy of −801 kJ/mol [30]. In both cases, the values are negative, indicating the spontaneity of these reactions. Experimentally it has been observed that there are Pt granulates on the surface of the coating on our devices, see Fig. 3. Furthermore, the spectral characteristics of the localised surface plasmons formed on the Pt granulates on the surface of the coating change in the presence of gaseous methane, see Figs. 6 and 7. Therefore considering the Pt

Table 1
A summary of the major components observed in the thin film coatings.

Sample	% atomic concentration					Pt Binding Energy $4f^7$
	C	O	Pt (Metalic)	Zn (ZnO)	Ge (GeO_2)	
ZnO/Pt thin Film	56	18.2	17.2	8.7	–	70.7 eV
UV processed ZnO/Pt thin film	23.4	26.5	28.3	20.4	1.5	70.8 eV
Platinum Control	–	–	100	–	–	71.0 eV

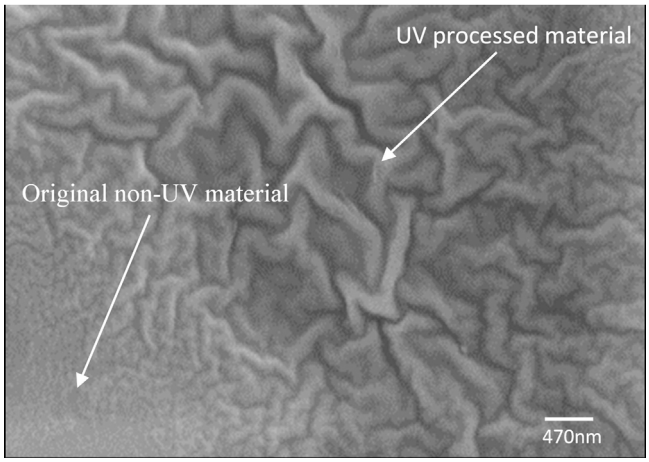

Fig. 8. Field-emission scanning electron microscopy on the Zn/Pt matrix coating showing a typical large field view of the surface with both UV and non-UV processed regions.

initial and final state:

$$2Pt : O_2^- + CH_4 \rightarrow [2Pt : O_2^- + C'H_3 + 'H] \rightarrow 2H_2O + CO_2 + 2Pt, \quad (1)$$

The authors realise that this is a simplified view and that the true reaction process will be complicated by the presence of Pt on the ZnO. It is known that other alkane gases react with O_2^- molecules with Pt acting as a catalyst, but for most of the alkane gases this occurs above room temperatures (20 °C–30 °C) [1–3,15,16]. Moreover, considering the ZnO thin film's sensitivity to methane and ethane there has been reported work [31] showing significantly higher sensitivity for methane than ethane over a nominal temperature range of 20 °C–60 °C, which is reasonably consistent with our experimental observations: the fact that we see marked differences between the methane and the ethane results, in Figs. 6a, b and 7. This is reasonable consistent with the fact that for a given catalyst the energy required for the activation of a C—H bond within each molecule is different indicating different temperature requirements for the reaction [32,33]. In addition, to complicate matters more, it is known that the type and physical state of the catalyst effects the reaction of the molecules [33], and the surface topology of this sensing material is complex due to the fabrication procedure and plays an important role in the overall reaction to methane. The UV processed sensing platform had a different surface topology, see Fig. 8 which produced a difference in the experimental results, which can be seen by inspecting Figs. 6 and 7.

Furthermore the methane Gibbs free energy change of formation (G_f^θ) has the largest negative value of $-50.8\,kJmol^{-1}$ (for example compared to ethane which has a G_f^θ value of $-32.9\,kJmol^{-1}$ both at a temperature of 25 °C [30,34]) suggesting that initial breakdown of the methane occurs more readily at lower temperatures than ethane which assists to promote the reaction. The authors suspect that the most significant factor is the ZnO having a higher sensitivity for methane working in conjunction with the Pt catalyst which promotes this reaction more favourably than for ethane or the rest of the alkane gases.

The result of such a reaction will yield an overall reduction in the density of the electrons on the surface of the Pt in the presence of methane. It is known that the electron density is directly proportional to the effective permittivity of the dielectric material. Therefore, considering the above reaction, within the immediate surrounding environment of the surface of the Pt granulates where the O_2^- molecules reside; these O_2^- molecules will be stripped away from the platinum during the above reaction in the presence of methane, which doesn't occur for the other alkane gas. This stripping away of O_2^- would cause a depletion in electron density in close proximity to the Pt granules' surface, creating a reduction in the surrounding medium's effective permittivity, which is related to the optical refractive index, which is in turn directly related to the phase match condition of the surface plasmons in the spectral domain [35]. The permittivity reduction leads to the opposite wavelength shift that would be expected with an increase in the bulk refractive index of the medium surrounding the Pt granulates (an increase in the effective permittivity).

To help confirm the mechanism for the opposite wavelength shift that was observed with methane, XPS was performed on the thin film coating before and after UV processing along with a control platinum test sample; the results are shown in Fig. 9 and Table 1. Inspecting the binding energy curves for the ZnO/Pt UV processed material and the pristine ZnO/Pt samples and comparing with a pure Pt control sample, there is a small difference in the binding energies of the $4f^7$ orbital of 0.2 and 0.3 eVs, respectively. This difference between the Pt and the ZnO/Pt samples is close to the resolution of the equipment used but it does suggest that there is a weak interaction occurring and that the Pt: O_2^- bond could be the origin for this difference. Moreover, the binding energy is less in the non-UV processed coating than for the UV processed one, thus less energy is required for the reaction to occur than for the UV processed coatings. This would appear in the experimental characterisation of the UV processed coatings, having less sensitivity to methane than the non-UV coating; this spectral behaviour was observed.

4. Discussion

When comparing this optical sensing platform to other photonic methane sensing schemes in the literature, there are several types to be considered. One is the spectroscopic/interferometric techniques that are based upon absorption lines at ~1650 nm or ~1330 nm [4,6] for which such systems have reported a limit of detection of 50 ppm. However, these spectroscopic techniques require long integration times of around a minute and the sensing elements are large in size ranging from 5 cm to 40 cm. Moreover, these spectroscopic techniques are mostly operating in the range of 1–5% volume and yield resolutions of 0.01%–0.05%. Whilst the spectroscopic techniques offer good performance they only operate over a limited range compared to the device being demonstrated here that delivers a useable range from 1% to 100%, which covers the lower explosive limit LEL (4.4%) and upper explosive limit (15%). At the higher concentrations there appears to be some nonlinearity in

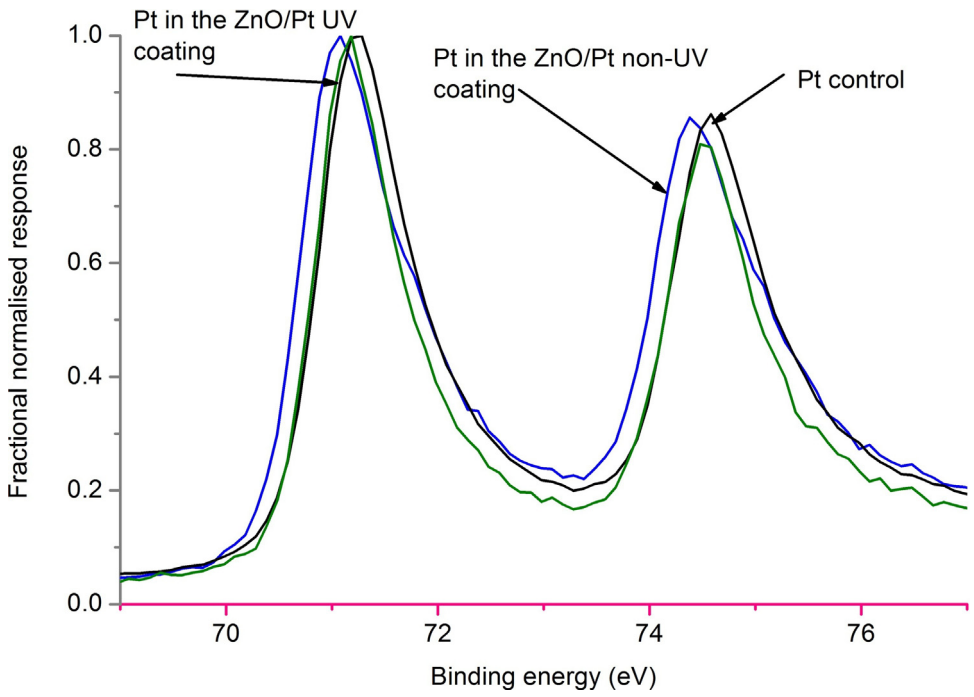

Fig. 9. Experimental results from x-ray photon-emission spectroscopy (a) typical spectra of the Pt $4f^7$ electron orbital of the ZnO/Pt and UV processed ZnO/Pt samples compared to a metallic Pt control.

the response to increasing concentration of methane, which may be indicative of a saturation effect occurring.

The spectroscopic/interferometric techniques are complicated, physically bulky and they generally are not viable for multiplexing and are costly to manufacture compared to the device reported here, which is small, potentially cheaper and can be multiplexed. Furthermore, in the spectroscopic systems, the sample cells may produce spurious reflections and spurious interferometers with contrast ratios of similar magnitude to the signal being detected, which can be a significant problem [7]; that is not an issue with the demonstrated plasmonic sensing platform.

The interaction of gases with evanescent optical fields, such as is provided by long period gratings [13], has had some limited success detecting ammonia but not yet methane and using photonic crystal fibre generates other problems such as the time it takes to fill the holes along with connectorisation to more conventional fibre optic components. There are other evanescent optical field sensors [14,36,37] that operate well below LEL at 0.1%, however evanescent sensors use a methane absorption line at 1651 nm, thus multiplexing such sensors working at the same wavelength complicates the required interrogation scheme. Furthermore, these evanescent sensors are based upon a long length of D-shaped fibre (1 m) with an exposed core, this length of fibre is mechanically fragile.

Conventional electrically based MOS devices generally have low sensitivity and poor chemical selectivity and have high energy consumption but potentially can be used for a wide range of target gases. They can also have short response times, long lifetimes and low manufacturing costs. The majority of these types of sensors work at elevated temperatures – typically 200–300 °C [1–3,38,39], which is a disadvantage compared to the plasmonic sensing platform in this work, which operates at room temperature and without any spark hazard to the sensed environment. Furthermore the conventional MOS sensors have issues with chemical selectivity and interference caused by other chemicals being present; for example, carbon dioxide in the sampled atmosphere can corrupt a sensor's performance [1,2,40].

The plasmonic device has been used with other alkane gases as well as carbon dioxide and has shown a distinctive specific spectral behaviour with methane that is not produced by the other gases. The explanation for this behaviour with regards carbon dioxide is because the sensing is done at room temperature and the carbon dioxide reaction needs elevated temperature to become significant [1,40,41]. Some work has been done to lower the operational temperature of electrical sensors by using a palladium–silver-activated ZnO surface [16] but they still require elevated temperatures of around 100 °C, thus having still a significant power footprint and again there are issues with regards to chemical selectivity and multiplexing capabilities. In terms of detection limits to methane of the MOS electrical sensors, they have similar or slightly lower detection limits along with similar sensitivities [1,38,41] to the plasmonic device.

5. Conclusions

In this paper we describe and demonstrate an optical sensing scheme that can detect changes in the optical properties of a metal oxide semiconductor (ZnO) in a multi-thin film matrix with platinum in the presence of the hydrocarbon gas methane. The operation of the device is based upon the interaction of near-infrared localised surface plasmons generated by platinum regions within a matrix of zinc oxide. A limit of detection of 2% by volume with concentrations from 0 to 12% at room temperature is demonstrated along with a selective chemical response to methane over carbon dioxide and the other alkane gases. This sensor yields an equivalent refractive index spectral sensitivity of 1.8×10^5 nm/RIU. The optical mechanism that is utilised within the sensing platform occurs without elevated temperatures, thus it is suitable for applications at ambient temperature. The non-electrical and passive mechanism makes it suitable for flammable and potentially explosive environments. Furthermore this sensing approach has potential and capabilities to be multiplexed to form sensing arrays.

The general comparison with alternative sensing approaches has shown that there are some major advantages with this optical sensing platform as a methane sensing scheme over the majority of techniques currently used. More importantly, the authors believe that this is the first time that the optical properties of MOS have been monitored to detect the presence of a specific gas. This single observation is a significant result, because MOSs have a potentially large number of target gases, thus offering a new paradigm for gas sensing using MOSs.

Acknowledgments

This work was financially supported by grants EP/J010413 and EP/J010391 for Aston University and University of Plymouth from the UK Engineering and Physical Sciences Research Council. The contribution of the authors is as follows: T. A. developed the original optical plasmonic gas sensor concept. T.A. modelled the behaviour, designed and performed experiments and analysed the data for the plasmonic devices. T.A., R.N., fabricated the plasmonic devices. T. A., G. B. L. and K.K. designed and performed experiments for gas sensing. V. K., P. B., R. N., B. S., J. S. and T.A. characterised the devices. T. A. developed the explanation for the sensor behaviour. The manuscript was written by T.A., R. N., K.K., D.J.W., B. S., J. S. and P.C. All authors discussed the results and commented on the manuscript. To access the data underlying this publication, please contact researchdata@aston.ac.uk., see http://doi.org/10.17036/researchdata.aston.ac.uk.00000276.

References

[1] P. Sumati, A. Maity, P. Banerji, S.B. Majumder, Qualitative and quantitative differentiation of gases using ZnO thin film gas sensors and pattern recognition analysis, Analyst 139 (7) (2014) 1796–1800.
[2] G. Fine, L.M. Cavanagh, A. Afonja, R. Binions, Metal oxide semi-conductor gas sensors in environmental monitoring, Sensors 10 (6) (2010) 5469–5502.
[3] L. Yanfang, L. Chang, Y. Zhao, X. Meng, Y. Wei, X. Wang, J. Yue, T. Liu, A fiber optic methane sensor based on wavelength adaptive vertical cavity surface emitting laser without thermoelectric cooler, Measurement 79 (2016) 211–215.
[4] N. Jiasheng, J. Chang, T. Liu, Y. Li, Y. Zhao, Q. Wang, Fiber methane gas sensor and its application in methane outburst prediction in coal mine, in: IEEE Optical Fiber Sensors Conference, APOS'08, Asia-Pacific, Chengdu, China, 2008, pp. 1–4.
[5] D.A. Lashof, D.R. Ahuja, Relative contributions of greenhouse gas emissions to global warming, Nature 344 (1990) 529–553.
[6] L. Geng-Chiau, L. Hon-Huei, A.H. Kung, A. Mohacsi, A. Miklos, P. Hess, Photoacoustic trace detection of methane using compact solid-state lasers, J. Phys. Chem. A 104 (45) (2000) 10179–10183.
[7] L. Bin, C. Zheng, H. Liu, Q. He, W. Ye, Y. Zhang, J. Pan, Y. Wang, Development and measurement of a near-infrared CH_4 detection system using 1.654 μm wavelength-modulated diode laser and open reflective gas sensing probe, Sens. Actuators B 225 (2016) 188–198.
[8] B. Culshaw, G. Stewart, F. Dong, C. Tandy, D. Moodie, Fibre optic techniques for remote spectroscopic methane detection—from concept to system realisation, Sens. Actuators B 51 (1998) 25–37.
[9] L.R. Brown, Empirical line parameters of methane from 1.1 to 2.1 μm, J. Quant. Spectrosc. Radiat. Transfer 96 (2) (2005) 251–270.
[10] L. Xiao, S. Cheng, H. Liu, S. Hu, D. Zhang, H. Ning, A survey on gas sensing technology, Sensors 12 (7) (2012) 9635–9665.
[11] P. Jacquinot, B. Müller, B. Wehrli, P.C. Hauser, Determination of methane and other small hydrocarbons with a platinum–nafion electrode by stripping voltammetry, Anal. Chim. Acta 432 (1) (2001) 1–10.
[12] L.H. Yeuk, W. Jin, C. Shi, H.L. Ho, D.N. Wang, S.C. Ruan, Design and modeling of a photonic crystal fiber gas sensor, Appl. Opt. 42 (18) (2003) 3509–3515.
[13] S. Zheng, M. Ghandehari, J. Ou, Photonic crystal fiber long-period grating absorption gas sensor based on a tunable erbium-doped fiber ring laser, Sens. Actuators B 223 (2016) 324–332.
[14] F.A. Muhammad, H.S. Al-Raweshidy, J.M. Senior, Compensation for surface contamination with D-fibre sensor, Sens. Actuators B 40 (1) (1997) 59–63.
[15] M. Parta, A. Halder, Effect of initialization time on application potentiality of a ZnO thin film based LPG sensor, Mater. Res. 12 (3) (2009) 329–332.
[16] S. Ghosh, C. RoyChaudhuri, R. Bhattacharya, H. Saha, N. Mukherjee, Palladium–silver-activated ZnO surface: highly selective methane sensor at reasonably low operating temperature, ACS Appl. Mater. Interfaces 6 (6) (2014) 3879–3887.
[17] T. Allsop, R. Arif, R. Neal, K. Kalli, V. Kundrát, A. Rozhin, P. Culverhouse, D.J. Webb, Photonic gas sensors exploiting directly the optical properties of hybrid carbon nanotube localized surface plasmon structures, Light: Sci. Appl. 5 (2016) e16036.
[18] I. Bennion, J.A.R. Williams, L. Zhang, K. Sugden, N.J. Doran, UV-written in-fibre bragg gratings, Opt. Quantum. Electron. 289 (2) (1996) 93–135.
[19] W. Kiyotaka, M. Kitabatake, H. Adachi, Thin Film Materials Technology: Sputtering of Control Compound Materials, Springer-Verlag Berlin Heidelberg, New York, USA, 2004.
[20] P.R. Naira, M.A. Alam, Performance limits of nanobiosensors, Appl. Phys. Lett. 88 (2006) 233120.
[21] T. Allsop, R. Neal, M. Dvorak, K. Kalli, A. Rozhin, D.J. Webb, Physical characteristics of localized surface plasmons resulting from nano-scale structured multi-layer thin films deposited on D-shaped optical fiber, Opt. Express 21 (16) (2013) 18765–18776.
[22] S. Patskovsky, A.V. Kabashin, M. Meunier, J.H.T. Luong, Properties and sensing characteristics of surface-plasmon resonance in infrared light, JOSAA 20 (8) (2003) 1644–1650.
[23] T. Allsop, R. Neal, S. Rehman, D.J. Webb, D. Mapps, I. Bennion, Generation of infrared surface plasmon resonances with high refractive index sensitivity utilizing tilted fiber Bragg gratings, Appl. Opt. 46 (26) (2007) 5456–5460.
[24] C. Caucheteur, T. Guo, J. Albert, Review of plasmonic fiber optic biochemical sensors: improving the limit of detection, J. Anal. Bioanal. Chem. 407 (14) (2015) 3883–3897.
[25] M. Weber, Handbook of Optical Materials, CRC PRESS, 2002.
[26] R. Rollefson, R. Havens, Index of refraction of methane in the infra-red and the dipole moment of the CH bond, Phys. Rev. 57 (8) (1940) 710.
[27] Q. Qi, T. Zhang, Q. Yu, R. Wang, Y. Zeng, L. Liu, H. Yang, Properties of humidity sensing ZnO nanorods-base sensor fabricated by screen-printing, Sens. Actuators B 133 (2008) 638–643.
[28] E. Palik, Handbook of Optical Constants of Solids, vol. II, Academic Press Inc, London, 1985.
[29] E.H. Ale, E. Jamshidi, Kinetic study of zinc oxide reduction by methane, Chem. Eng. Res. Des. 79 (1) (2001) 62–70.
[30] V. Havran, M.P. Dudukovicí, C.S. Lo, Conversion of methane and carbon dioxide to higher value products, Ind. Eng. Chem. Res. 50 (12) (2011) 7089–7100.
[31] P. Nunes, E. Fortunato, Thin film combustible gas sensors based on Zinc Oxide, MRS Online Proc. Libr. Arch. 666 (2001).
[32] S.Y. Arndt Aksu, M. Driess, R. Schomäcker, The catalytic activity of zinc oxides from single source precursors with additives for the C–H acitivation of lower alkanes, Catal. Lett. 131 (1–2) (2009) 258–265.
[33] H. Arnold, F. Döbert, J. Gaube, G. Ertl, H. Knözinger, F. Schüth, J. Weitkamp, in: G. Ertl, H. Knözinger, J. Weitkamp (Eds.), Handbook of Heterogeneous Catalysis, 2008, pp. 2165–2186.
[34] W.M. Haynes (Ed.), CRC Handbook of Chemistry and Physics, CRC press, 2014.
[35] H. Raether, Surface Plasmons on Smooth and Rough Surfaces and on Gratings, Academic, New York, 1997.
[36] H. Tai, T. Yoshino, H. Tanaka, Fiber-optic evanescent-wave methane-gas sensor using optical absorption for the 3.392-μm line of a He–Ne laser, Opt. Lett. 12 (6) (1987) 437–439.
[37] G. Stewart, W. Jin, B. Culshaw, Prospects for fibre-optic evanescent-field gas sensors using absorption in the near-infrared, Sens. Actuators B 38 (1) (1997) 42–47.
[38] P. Mitra, A.K. Mukhopadhyay, ZnO thin film as methane sensor, Bull. Polish Acad. Sci. Tech. Sci. 55 (3) (2007) 281–285.
[39] P. Bhattacharyya, P.K. Basu, H. Saha, S. Basu, Fast response methane sensor using nanocrystalline zinc oxide thin films derived by sol–gel method, Sens. Actuators B 124 (1) (2007) 62–67.
[40] S. Basu, P.K. Basu, Nanocrystalline metal oxides for methane sensors: role of noble metals, J. Sens. (2009), 861968.
[41] T.P. Chen, S.P. Chang, F.Y. Hung, S.J. Chang, Z.S. Hu, K.J. Chen, Simple fabrication process for 2D ZnO nanowalls and their potential application as a methane sensor, Sensors 13 (3) (2013) 3941–3950.

Biographies

Dr Thomas Allsop graduated from Queen Mary College with a Hons degree in Physics and Astrophysics in 1986, continued studies with a M.Sc. in optoelectronics from Newcastle University followed by a PhD in optoelectronics/photonics from University of Plymouth in 1998. Since then worked at Aston University in Aston Institute of Photonics Technologies and Photonics Research Group for a total of 17 years with current position of senior research fellow specialising in biomedical optics and biophotonics (biochemical sensors and biosensors). Along with a consultative role in the field of astrophotonics for the institute of astrophysics in Potsdam, Germany. These activities have resulted in over a 120 publications (with 80 being the lead author) and resulted in 12 international patents in the field of photonics, biomedical optics, opto-chemical sensing and bio-photonics.

Dr Vojtěch Kundrat, PhD in Nanotechnology Science from Aston University in 2015, several publications in the field of nanodiamond fabrication and spectroscopy. Now working in Industry.

Dr Kyriacos Kalli, is an Associate Professor in the Department of Electrical Engineering and Information Technology. He received the B.Sc. (Hons) in Theoretical Physics (1988) and Ph.D. in Physics (1992) from the University of Kent, UK, where he studied linear and non-linear phenomena in optical fibres. In 1993 he was a visiting research scholar at Virginia Polytechnic Institute and State University, USA, study-

ing optical fibre sensors. From 1994 – 1996 he lectured and undertook research at the University of Kent into the use of fibre Bragg gratings in multiplexed sensor arrays and Raman spectroscopy. At the University of Cyprus (1996 onwards) he was engaged in research into integrated gas flow and gas sensors based on porous silicon micromachining, fluorescence spectroscopy, and non-destructive evaluation of semi-conductors. From 2001 he was a lecturer at the Higher Technical Institute, where he created and headed the Nanophotonics Research Laboratory. His research interests are in Bragg grating and optical fibre sensors, photonic switching devices, multiplexing of optical sensors and laser material interactions. Dr. Kalli is a member of the Institute of Physics (C.Phys.), Optical Society of America and Institute of Electrical and Electronics Engineers. These activities have resulted in over a 200 publications.

Dr Graham B. Lee, PhD in photonics with emphasis on femtosecond laser material interaction and applications from Aston University in 2015, several publications in the field of Femtosecond inscription and micro-machining. Now working in Industry.

Ron Neal, A Senior Research Fellow and Former Senior lecturer in Photonics and optoelectronics in the School of Computing, Electronics and Mathematics at the University of Plymouth. Current research interests are photonics, biomedical optics, opto-chemical sensing and bio-photonics. These activities have resulted in over a 30 publications.

Peter Bond, Technical Specialist and experimental officer in the School of Computing, Electronics and Mathematics at the University of Plymouth. Main research interests are based on the effects of metal toxicity on the growth and ultrastructure of marine algae, but the EM Centre has links with many and varied research groups both within the university and with local collaborating institutes and research centres. These activities have resulted in over a 15 publications.

Dr Baogui Shi, Research Associate working in Midlands Surface Analysis at Aston University, specialising surface Tribology obtained his PhD in 2002. These activities have resulted in over a 15 publications.

Prof John Sullivan, Professor in the field of Surface Science at Aston University with research interests in surface-particle interactions: electron and ion spectrometry, ion optics. Also the director of Midlands Surface Analysis. These activities have resulted in over a 120 publications.

Dr Phil Culverhouse, Associate Professor (Senior Lecturer) in Computer Vision & Robotics in School of Computing, Electronics and Mathematics at the University of Plymouth, obtained PhD in Engineering from Plymouth in 1994. Research interest are Natural Object Categorisation, Machine vision, Expert performance, in situ plankton recognition. Along with a leader in the Robotics and Intelligent Systems Research Group with over 50 publications.

David. J. Webb, University of Oxford (BA in Physics at St. Catherine's) and the University of Kent (PhD in Physics) and I have also spent time as a postdoc in the Department of Engineering Science at Oxford and in industry with GEC Research in Great Baddow, Chelmsford, Aston University as Reader in Photonics in May 2001 and was promoted to Professor in June 2012 and Deputy Director of the Aston Institute of Photonic Technologies. Research interests in the field of photonics, working in the areas of non-linear optics and optical fibre sensors and devices. These activities have resulted in over a 220 publications.